Oxidation of pure and potassium-doped NiTi shape memory surface: A density functional theory investigation

K. N. Nigussa and J. A. Støvneng*
Department of Physics, NTNU, N-7491 Trondheim, Norway
(Received 2 July 2010; revised manuscript received 11 October 2010; published 1 December 2010)

The oxidation of Ti-terminated NiTi surfaces is investigated with density functional theory. The surfaces considered are (001) and (110) of the austenite phase (B2) and (010) of the martensite phase (B19′). The favored adsorption sites for atomic oxygen are fourfold hollow on B2 (001), and twofold bridged between two surface Ti atoms on B2 (110) and B19′ (010). Adsorption of one oxygen molecule per surface Ti atom results in the formation of a rutilelike protective layer of TiO_2. The oxidation results in outward and inward movement of surface Ti and Ni atoms, respectively, signaling depletion of Ni atoms from the surface region. Substitution of Ni by K near the surface is found to enhance the formation of TiO_2 at the expense of TiO, and increase the stability and facilitate the growth of thicker layers of titanium oxides on the NiTi surfaces. This is of importance for the biofunctionality of the alloy.

DOI: 10.1103/PhysRevB.82.245401 PACS number(s): 73.20.At, 68.43.Fg

I. INTRODUCTION

NiTi alloy with equiatomic composition (Ti-50 at. % Ni) is known to be a shape memory material.[1,2] By application of force or temperature, it undergoes a change in structure from the parent austenite phase (B2) to the martensite phase (B19′) or vice versa.[2] If an impact is applied and released in one of the phases, the original shape would be recovered in the other phase. The intermetallic composition is also being tailored for various purposes by varying the Ni content in the binary alloy or making a ternary alloy by replacing some of the Ni atoms with other transition metals.[1,3] However, this will typically lead to significant loss of the initial shape memory property. The alloy has also been confirmed to be biocompatible with body tissue, and as a consequence it is being used in various medical applications including dentistry, orthopaedics, and vascular surgery.[1,4,5]

The best biofunctionality of the NiTi alloy is achieved when the presence of Ni atoms at the surface is minimized. This follows from numerous reports showing that high amounts of Ni atoms at the surface could result in a leakage to the body and cause hazards.[6,7] Appropriate surface treatment or coating is widely seen as the best remedy to this problem. Titanium oxides including TiO and TiO_2 are in general considered to offer good chemical stability and biocompatibility.[8–10] It is noted that TiO_2 is the most stable form and TiO is a transient phase to TiO_2. Under ultrahigh-vacuum conditions, TiO_2 is found to dominate at low temperatures and TiO is found to dominate at high temperatures.[8] Under high-pressure conditions, TiO dominates at low temperatures and TiO_2 dominates at high temperatures.[9,10] Several studies have been devoted to quantitative characterization of surface oxidation, where exposure of the surface to a sufficient amount of oxygen was found to result in the formation of a TiO_2 protective layer.[8,11,12] In addition to increasing the corrosion resistance of the NiTi alloy surface,[13] a TiO_2 layer is believed to promote its biofunctionality.[14]

The B2 phase of NiTi has a CsCl type structure and exists at temperatures higher than about 330 K.[15,16] The B2 phase has also been found in several Ti-based alloys[17,18] and even in NiTi-based ternary alloys.[19,20] However, the B19′ phase with monoclinic structure is unique to the NiTi alloys and exists at temperatures lower than about 320 K. The B19′ phase is sensitive to the composition of the alloy, and as a consequence, Ti- and NiTi-based alloys with different composition histories have different martensite transformation processes and martensite start temperatures (M_s).[8,15–17,19–21] The (near) equiatomic NiTi alloy attracts attention because it undergoes the structural transformation from B2 to B19′ in just one step (i.e., with no other intermediate structure in between).[1,22] Increasing the Ni content or alloying with a third transition metal by replacing some of the Ni atoms, extends the number of steps to at least two, with an intermediate structure of rhombohedral *R* (Refs. 20 and 21) or orthorhombic (B19),[22] provided that the amount of Ni replacement is significant. When the amount of Ni replacement is small, the transformation occurs in just one step where the M_s temperature decreases slightly below 320 K, depending on the type of added transition metal.[23] However, it is not clear what health impact these transition metals have when used in alloys in medical implants. Alkali metals, typically Na and K, when present in small amounts, are known to be harmless for the body. They have been found to promote oxidation of semiconductor surfaces.[24] A recent experimental study[8] showed that the presence of a thin layer of K on the NiTi surface enhances the oxidation of surface Ti atoms to TiO_2.

In addition to the many experimental efforts carried out to characterize the oxide growth on NiTi, *ab initio* atomic level investigations have recently also been reported.[11,25,26] In the present work, we use density functional theory (DFT) to address the oxidation of selected surfaces of NiTi in the B2 and B19′ phases. On the basis of both experimental and theoretical reports, we focus on the (110) and (001) surfaces of B2 and the (010) surface of B19′. Coverages ranging from 0.5 to 2.0 oxygen atoms per surface Ti atom are explored, resulting in various TiO and TiO_2 surface layers that are conveniently compared with, and categorized in terms of, the corresponding clean titanium oxide surfaces. The influence of

exposing the NiTi surfaces to potassium is addressed by replacing near surface Ni atoms with K.

The paper is organized as follows: in Sec. II, details of the computational method are presented. In Sec. III, we report the results of our calculations. We close the paper with a discussion in Sec. IV and a conclusion in Sec. V.

II. COMPUTATIONAL METHODS

All calculations presented are based on DFT. The Kohn-Sham equations are solved within the generalized gradient approximation, using Vosko, Wilk, and Nusair's parametrization (VWN, Ref. 27) of the correlation energy within the local-density approximation (LDA), contribution and the PW91 (Ref. 28) gradient corrections to the exchange and correlation energy.

A slab type model with five layers of NiTi is used for the surface calculations. Three layers are constrained to the bulk geometry while two layers are allowed to relax together with the adsorbate (O or O_2). In most of our calculations, an adsorbate coverage of one or two oxygen atoms per surface Ti atom is being used. We refer to this as 1 ML O and 1 ML O_2 (ML=monolayer), respectively. In these calculations, prior to oxidation, the undoped (1×1) supercell contains five Ti and five Ni atoms. The influence of K (K doping) is modeled by replacing one Ni atom near the surface by K, i.e., the (1×1) supercell contains one K, five Ti, and four Ni atoms. A lower coverage of 0.5 O per surface Ti requires a (2×1) supercell with ten Ti and ten Ni atoms (undoped surface). The influence of K doping is also in this case modeled by replacing one near surface Ni by K, i.e., the supercell prior to oxygen adsorption consists of one K, ten Ti, and nine Ni atoms.

Calculations with (1×1) supercells are performed with the ADF/BAND program package.[29] The electronic wave functions are constructed as linear combinations of atomic orbitals.[30] The wave functions of the core electrons (O: 1*s*; K, Ti, Ni: 1*s*, 2*s*, 2*p*) are expressed in terms of Herman-Skillman-type numerical atomic orbitals (NAOs) whereas those of the valence electrons are described by one NAO plus two Slater-type orbitals, in what is called triple ζ quality. To allow for angular flexibility, two shells of higher angular momentum have been included in the basis set, i.e., triple ζ plus two polarization functions. Relativistic effects in a scalar form[31] have been included in the kinetic energy of the electrons. This typically lowers the energy by about 1 eV pr unit cell. Consequently, the calculated adsorption energies are not much affected (less than 0.1 eV) by including relativistic effects. The *k*-space integrations employ a quadratic tetrahedron method,[32] with the KSPACE parameter equal to 5. Depending on the degree of symmetry, the number of symmetry unique *k* points typically ranges from 15 to 34 in the slab calculations.[33]

Isolated adsorbates, O (atomic oxygen) and O_2 (molecular oxygen), were optimized in a cubic structure with lattice constant 15 Å. This is sufficient to avoid adsorbate-adsorbate interactions prior to adsorption. For both O and O_2, a triplet ground state is found, with a preference over the lowest singlet state of 1.52 eV and 1.16 eV, respectively, in reasonable agreement with experimental and theoretical values in the literature.[34,35] The reaction $O+O\rightarrow O_2$ is found to be exothermic by 6.83 eV with the chosen method. Except for the isolated adsorbates, all calculations presented in Sec. III are spin restricted (i.e., spin unpolarized). Test calculations allowing spin polarization indeed predict net atomic magnetization in some of the slab models, and typically, the surface Ti atoms are predicted to have the largest spin values, up to 1.4 μ_B. However, the energy differences between the spin restricted and spin unrestricted calculations are small (less than 0.5 eV), and will not affect the trends in our calculations. The relaxed geometries are also little influenced by this choice. Therefore, only spin restricted calculations have been included. For all the relevant bulk systems (B2 and B19′ NiTi and hcp Ti), the ground states possess no spin polarization.

With (2×1) supercells, i.e., for an adsorbate coverage of 0.5 oxygen atom per surface Ti, the computational time turned out to become prohibitively long with the ADF/BAND program. For these systems, the plane-wave-based DFT program DACAPO (Ref. 36) was used. In DACAPO, Vanderbilt[37] ultrasoft pseudopotentials are implemented, and relativistic effects are not taken into account. The comments above, concerning spin restricted vs spin unrestricted calculations, are equally valid when the DACAPO program is used for these systems, i.e., energy differences after geometry relaxation with and without allowance for spin polarization are below 0.5 eV, and geometry differences are negligible. In our DACAPO calculations, the triplet ground state of O and O_2 are favored by 1.96 eV and 1.10 eV, respectively, over the lowest singlet state, and the $O+O\rightarrow O_2$ reaction is exothermic by 5.59 eV.

In DACAPO, the system is always periodic in all three dimensions, so for the slab calculations, a vacuum layer of 10 Å is introduced to minimize artificial interactions between the slabs.[38] A *k*-point mesh of $4\times4\times1$ is used for the slab calculations. For the bulk crystals, a *k*-point mesh of $4\times4\times4$ is used. The *k* points are chosen based on the Monkhorst-Pack scheme.[39] The electron wave functions are expanded in plane waves with a cut-off energy of 400 eV.

Clearly, the adsorption energies calculated for (2×1) supercells with DACAPO cannot be directly compared with those calculated for (1×1) supercells with ADF/BAND. However, the DACAPO results do indicate certain trends concerning low (submonolayer) oxygen coverage.

We define the adsorption energy as

$$E_{ads} = -(E_{S+O} - E_S - E_O), \tag{1}$$

for adsorption of a single oxygen atom. The coverage is then 0.5 and 1.0 oxygen atoms per surface Ti, i.e., 0.5 and 1.0 ML O, respectively, for the (2×1) and (1×1) supercells. The adsorption energy is defined as

$$E_{ads} = -(E_{S+O_2} - E_S - E_{O_2}), \tag{2}$$

for adsorption of an oxygen molecule. This corresponds to a coverage of 1.0 and 2.0 oxygen atoms per surface Ti, i.e., 0.5 and 1.0 ML O_2, respectively, for the (2×1) and (1×1) supercells. Here E_{S+O}, E_{S+O_2}, E_S, E_O, and E_{O_2} are total energies,

TABLE I. Adsorption of oxygen on the B2 phase of Ti-terminated NiTi. In each case, one O atom or one O_2 molecule is adsorbed. $z_{Ti}-z_{Ni}$ is the (vertical) distance between the surface Ti layer and the first Ni layer below, and $\Delta z_{Ti\text{-}Ni}$ is the change in this distance upon oxidation of the surface, (both measured in angstrom). ΔQ is the total (Mulliken) charge gained by the adsorbate (number of gained electrons per O atom or O_2 molecule). E_{ads} is the adsorption energy per O atom or O_2 molecule (in electron volt).

Surface, supercell	Figure	Adsorbate	$z_{Ti}-z_{Ni}$	$\Delta z_{Ti\text{-}Ni}$	E_{ads}	ΔQ
(001), (1×1)	1(a) and 1(b)	O	1.89	0.39	8.87	0.88
(001), (1×1)	3(a) and 3(b)	O_2	2.52	1.02	8.00	1.30
(001), (1×1)	3(c) and 3(d)	O_2	2.85	1.35	8.17	1.42
(001), (2×1)		O	1.92	0.62	8.48	
(001), (2×1)		O_2	1.80	0.50	10.76	
(110), (1×1)	1(c) and 1(d)	O	0.62	0.48	8.30	0.70
(110), (1×1)	3(e) and 3(f)	O_2	1.12	0.98	7.52	1.41
(110), (1×1)	3(g) and 3(h)	O_2	0.90	0.76	6.76	1.31
(110), (2×1)		O	0.54	0.23	7.64	
(110), (2×1)		O_2	0.63	0.32	9.56	

per supercell, of surface with one adsorbed oxygen atom, surface with two adsorbed oxygen atoms, clean surface, and isolated atomic and molecular oxygen, respectively. A positive E_{ads} implies an exothermic reaction. The reader who prefers to refer E_{ads} to molecular oxygen also in the case of adsorption of a single oxygen atom, should subtract half of the calculated dissociation energy for molecular oxygen, 3.42 eV [2.80 eV for the DACAPO calculations with (2×1) supercells], from the energy values in Tables I–IV.

In ADF/BAND, atomic charges are calculated based on a Mulliken analysis. In addition, the electronic structure is discussed in terms of the partial density of states (PDOS) on Ti, O, and K atoms, at or near the surface. Whenever the adsorbate is O_2, the PDOS for oxygen represents a sum of the PDOS of the two O atoms in the supercell.

In the discussion of the surface structures that result from adsorption of oxygen on the various Ti-terminated NiTi surfaces, we have found it convenient to make comparison with TiO (rocksalt structure) and TiO_2 (rutile structure), and in particular with selected low-index surfaces of these oxides. The oxide layer grown on the three different NiTi surfaces that we have investigated, has a geometric and electronic structure that compares well with one particular *as cleaved* single layer of TiO or TiO_2. Hence, we categorize the grown oxides on NiTi accordingly. We justify this categorization by comparing the surface Ti and O PDOS of the grown oxide on NiTi with the Ti and O PDOS of the as cleaved single layers of TiO or TiO_2. Since rutile TiO_2 has a unit cell with two Ti and four O atoms, a "single layer of TiO_2" is a slab with a thickness given by the unit cell. Hence, the supercell of this slab contains two Ti and four O atoms. The Ti PDOS is for the Ti atom with coordination equal to the coordination of the Ti atom in the oxide grown on NiTi. The O PDOS is obtained by summing over the three oxygen atoms that are bonded to the chosen Ti atom, i.e., one of the four O atoms is not included in the PDOS sum.

Finally, in order to assess the calculated adsorption energies, it is of interest to compare oxidation of NiTi with the corresponding adsorption reactions on surfaces of pure Ti (hexagonal close-packed structure). For bulk hcp Ti, we have calculated lattice parameters $a=b=2.93$ Å and $c=4.67$ Å, which are subsequently used for obtaining slab geometries representing the (001) and the (110) surfaces of Ti. Oxide formation on NiTi will be compared with oxygen adsorption on the triangular Ti(001) and the rectangular Ti(110) surfaces.

TABLE II. Adsorption of oxygen on the B2 phase of K-doped Ti-terminated NiTi. In each case, one O atom or one O_2 molecule is adsorbed. $z_{Ti}-z_{Ni}$ is the (vertical) distance between the surface Ti layer and the first Ni layer below, and $\Delta z_{Ti\text{-}Ni}$ is the change in this distance upon oxidation of the surface, (both measured in angstrom). ΔQ is the total (Mulliken) charge gained by the adsorbate (number of gained electrons per O atom or O_2 molecule). E_{ads} is the adsorption energy per O atom or O_2 molecule (in electron volt).

Surface, supercell	Figure	Adsorbate	$z_{Ti}-z_{Ni}$	$\Delta z_{Ti\text{-}Ni}$	E_{ads}	ΔQ
(001), (1×1)	5(a) and 5(b)	O	7.95	−0.15	9.67	0.98
(001), (1×1)	7(a) and 7(b)	O_2	8.55	0.44	9.68	1.47
(110), (1×1)	5(c) and 5(d)	O	2.01	0.27	9.23	0.91
(110), (1×1)	7(c) and 7(d)	O_2	1.99	0.25	10.94	1.75
(110), (2×1)	5(e) and 5(f)	O	0.34	0.16	7.35	
(110), (2×1)	5(g) and 5(h)	O	0.29	0.11	8.99	

TABLE III. Adsorption of oxygen on the B19′ phase of Ti-terminated NiTi. In each case, one O atom or one O_2 molecule is adsorbed. $z_{Ti}-z_{Ni}$ is the (vertical) distance between the surface Ti layer and the first Ni layer below, and $\Delta z_{Ti\text{-}Ni}$ is the change in this distance upon oxidation of the surface, (both measured in angstrom). ΔQ is the total (Mulliken) charge gained by the adsorbate (number of gained electrons per O atom or O_2 molecule). E_{ads} is the adsorption energy per O atom or O_2 molecule (in electron volt).

Surface, supercell	Figure	Adsorbate	$z_{Ti}-z_{Ni}$	$\Delta z_{Ti\text{-}Ni}$	E_{ads}	ΔQ
(010), (1×1)	9(a) and 9(b)	O	0.95	0.67	8.01	0.65
(010), (1×1)	9(c) and 9(d)	O_2	1.71	1.43	7.49	1.42
(010), (2×1)		O	0.70	0.32	7.54	

III. RESULTS

A. Adsorption of oxygen on the B2 phase of NiTi

1. Bulk B2 NiTi and its low index surfaces

The bulk modulus of the B2 phase of NiTi is estimated from a Birch fit[40] to be 160.7 GPa. This is in good agreement with experimental [140.3 GPa (Ref. 41)] and calculated [157.8 GPa (Ref. 42)] values. The lattice constant is calculated to be 3.02 Å, in good agreement with the experimental value of 3.00 Å.[16]

Cleavage of the crystal along planes that result in (001) and (111) surfaces will inevitably lead to both Ni and Ti terminated surfaces. However, since oxygen preferably reacts with Ti, only the Ti-terminated surfaces are considered here. The as cleaved (110) surface has equal amounts of Ni and Ti atoms in the surface layer. However, upon geometry relaxation, the Ti atoms move outward and the Ni atoms move inward, resulting in an essentially Ti terminated surface. This is consistent with previously reported calculations.[11,25]

For the three Ti terminated surfaces, we find that the (001) surface is 0.35 eV more stable than the (110) surface and 1.64 eV more stable than the (111) surface. These values are based on total energies per supercell (i.e., per Ni_5Ti_5). Since the supercell surface area is smallest for the (001) and largest for the (111) surface, an evaluation of surface energies per unit area reveals the highest stability for the (110) surface and approximately equally stable (001) and (111) surfaces. In this work, we have limited ourselves to investigating oxidation of the (001) and (110) surfaces of the B2 phase. In Sec. II, we discuss the undoped NiTi surfaces. In Sec. III, we study the effects of potassium doping, i.e., substitution of near surface Ni atoms by K.

2. Oxygen adsorption on undoped B2 NiTi (001) and (110)

Both the (001) and the (110) surfaces of B2 NiTi interact strongly with oxygen. The calculated adsorption energies are large (in the range 7–11 eV), both for atomic and molecular oxygen, and both for low and high oxygen coverage (see Table I). These values are comparable to the heat of formation of TiO_2, 9.9 eV.[43]

On the (001) surface, at coverage (up to) one O per surface Ti, i.e., 1 ML O, oxygen adsorbs most favorably at the fourfold hollow site where it is bonded to four Ti atoms [Figs. 1(a) and 1(b)]. The adsorbed oxygen has equal bond distance 2.09 Å to each Ti atom. It is natural to categorize the grown surface layer as TiO(001), and we will call the structure TiO(001)/NiTi(001). A corresponding notation will be used in the following. In Fig. 2, the electronic structure of the oxide layer in TiO(001)/NiTi(001) is compared with a single layer of TiO(001), as cleaved from the bulk TiO crystal. Here, the PDOS is plotted for the Ti and O atoms in the surface layer of TiO(001)/NiTi(001), Fig. 2, (II), as well as for the single layer of TiO(001), Fig. 2, (III). Both the Ti and O PDOS curves are indeed very similar in Fig. 2, (II) and (III). The calculated Mulliken charges on oxygen are also similar, 0.88*e* for TiO(001)/NiTi(001) and 1.01*e* for the single layer of TiO(001).

The adsorption energy of 8.87 eV suggests the formation of strong Ti-O bonds. In comparison, for the adsorption of atomic oxygen in the threefold hollow site on the (001) surface of hcp Ti, we find an adsorption energy of 8.02 eV. In other words, a stronger oxide seems to be formed on the NiTi alloy than on the pure Ti crystal. This difference may be ascribed to weaker bonds between Ti and Ni atoms in the alloy than between Ti atoms in the Ti crystal. It appears that the presence of Ni below the Ti surface stabilizes the grown oxide layer without affecting its electronic structure significantly.

Increasing the coverage of oxygen to 1 ML O_2 leads to the formation of one TiO_2 layer on the parent NiTi(001) substrate. The most stable structures are shown in Figs. 3(a) and 3(b) and Figs. 3(c) and 3(d), for which the adsorption energies are 8.00 and 8.17 eV, respectively. Common to the

TABLE IV. Adsorption of oxygen on the B19′ phase of K-doped Ti-terminated NiTi. In each case, one O atom or one O_2 molecule is adsorbed. $z_{Ti}-z_{Ni}$ is the (vertical) distance between the surface Ti layer and the first Ni layer below, and $\Delta z_{Ti\text{-}Ni}$ is the change in this distance upon oxidation of the surface, (both measured in angstrom). ΔQ is the total (Mulliken) charge gained by the adsorbate (number of gained electrons per O atom or O_2 molecule). E_{ads} is the adsorption energy per O atom or O_2 molecule (in electron volt).

Surface, supercell	Figure	Adsorbate	$z_{Ti}-z_{Ni}$	$\Delta z_{Ti\text{-}Ni}$	E_{ads}	ΔQ
(010), (1×1)	11(a) and 11(b)	O	2.00	0.05	9.00	0.92
(010), (1×1)	11(c) and 11(d)	O_2	2.38	0.42	12.63	1.73

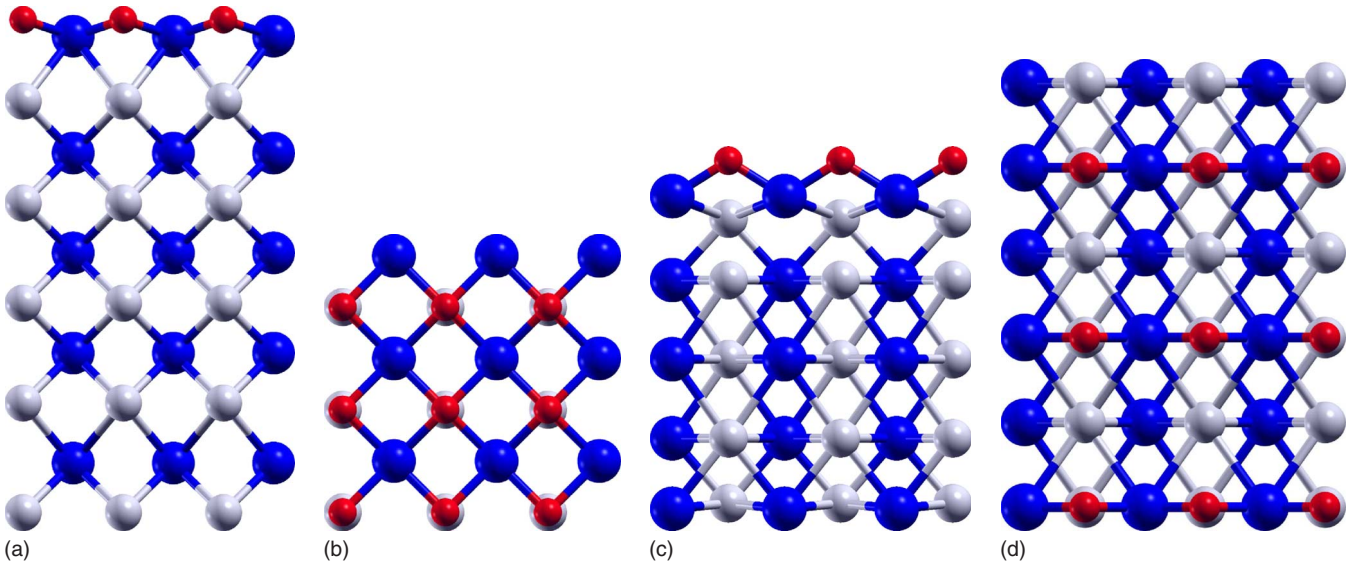

FIG. 1. (Color online) Adsorption of 1 ML O on B2 NiTi; (a) and (b) side and top view, fourfold hollow site on the (001) surface; (c) and (d) side and top view, twofold bridge site on the (110) surface. Colors (size, grayscale): Ti-blue (large gray), O-red (small, gray), Ni-white (large, white).

two geometries is the O atom in the fourfold hollow site. The second O atom is located on top of Ti in Figs. 3(a) and 3(b) whereas in Figs. 3(c) and 3(d) it is in a bridging position between two Ti atoms. In Figs. 3(a) and 3(b), the Ti-O bond lengths are 2.14 Å and 1.61 Å for O in the fourfold hollow site and on top of Ti, respectively. In Figs. 3(c) and 3(d), the Ti-O bond lengths are 2.25 Å and 1.83 Å for O in the fourfold hollow site and in the twofold bridging site, respectively.

Whereas the adsorption of 1 ML O on NiTi(001) clearly suggested a comparison with TiO(001), similar comparisons with specific surfaces of TiO_2 are in general less obvious. However, on the basis of the coordination of the Ti and O atoms involved, the oxide layers formed in Figs. 3(a) and 3(b), and Figs. 3(c) and 3(d), are best categorized as $TiO_2(100)$ and $TiO_2(110)$, respectively. As shown by Perron *et al.*,[44] the $TiO_2(110)$ surface contains Ti(5), Ti(6), and bridging O(2) and O(3). Here, Ti(5) means fivefold coordinated Ti, etc. The $TiO_2(100)$ surface contains Ti(5) bonded to bridging O(2) at the surface and subsurface O(3). The surface structures in Figs. 3(a) and 3(b), and Figs. 3(c) and 3(d) have Ti(5) and Ti(6), respectively. Hence, the suggested categorization. In Fig. 2, (IV) and (V), the surface Ti and O PDOS are plotted for $TiO_2(110)/NiTi(001)$, i.e., the structure in Figs. 3(c) and 3(d), and for a single (as cleaved) layer of $TiO_2(110)$, respectively. [Actually, Ti_2O_4, see Sec. II for a description of which Ti and O atoms contribute to the PDOS plotted in Fig. 2, (V).] The comparison is perhaps not quite as evident as in the case of TiO(001)/NiTi(001). However, both for O and Ti, the PDOS curves reveal similar profiles, in particular below the Fermi level. A comparison between the structure in Figs. 3(a) and 3(b) and a single layer of $TiO_2(100)$ (not included here) reveals corresponding similarities in the PDOS curves.

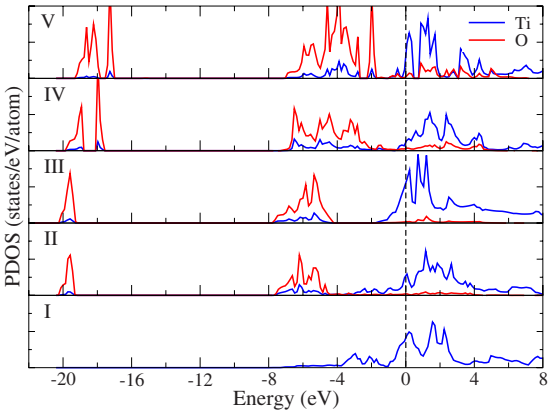

FIG. 2. (Color online) Partial density of states of Ti and O atoms: (I) clean Ti-terminated B2 NiTi(001) surface; (II) I+1 ML O adsorbed [Figs. 1(a) and 1(b)]; (III) one layer of TiO(001); (IV) I+1 ML O_2 adsorbed [Figs. 3(c) and 3(d)]; (V) one layer of $TiO_2(110)$.

Note the reduced value of the surface Ti PDOS at the Fermi level as a result of the oxidation, i.e., going from clean B2 (001) NiTi in Fig. 2, (I) via a coverage of 1 ML O in Fig. 2, (II) to a coverage of 1 ML O_2 in Fig. 2, (IV), where a layer of TiO_2 has formed on the surface. This is a general trend in all our calculations, and a clear signature of the reduced metallic character of the surface, as one would expect. A similar effect was pointed out by Nolan *et al.*[25]

As with atomic oxygen, we find significantly higher adsorption energies for dissociative adsorption of molecular oxygen on NiTi(001) than on the (001) surface of Ti. Adsorption of 1 ML O_2 on the Ti(001) surface is exothermic by only 3.37 eV per oxygen molecule. This, again, underscores the catalytic role played by Ni atoms, due to their relative inertness toward oxygen.

On the B2 NiTi(110) surface, at a coverage of one O per surface Ti (1 ML O), oxygen preferably adsorbs in a twofold bridge site between two Ti atoms, as shown in Figs. 1(c) and 1(d).[45] The Ti-O bond distance is 1.84 Å. We categorize the

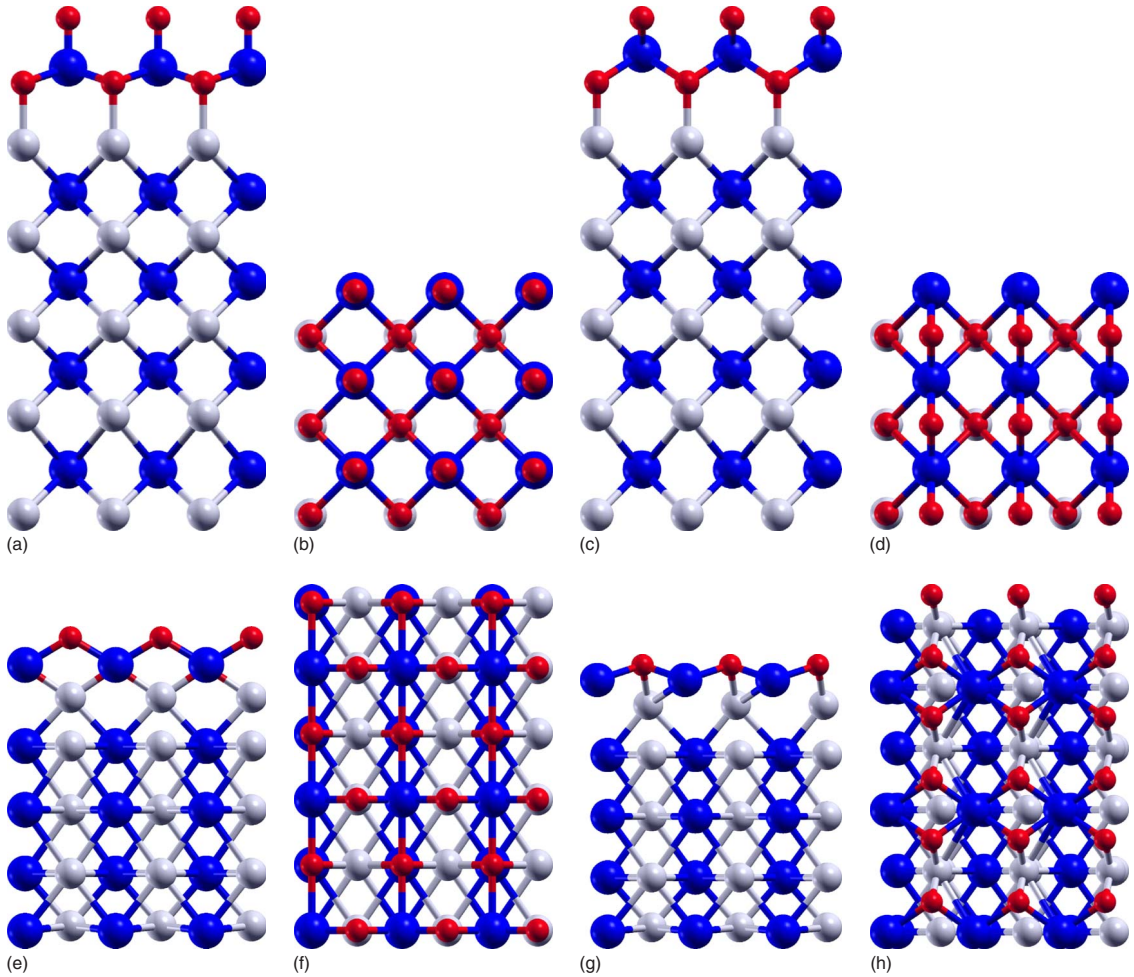

FIG. 3. (Color online) Adsorption of 1 ML O_2 on B2 NiTi; (a) and (b) side and top view, hollow and top sites on the (001) surface; (c), and (d) side and top view, hollow and bridge sites on the (001) surface; (e) and (f) side and top view, bridge and in-plane sites on the (110); (g) and (h) side and top view, bridge and bridge sites on the (110) surface. Colors (size, grayscale): Ti-blue (large, gray), O-red (small, gray), Ni-white (large, white).

grown surface layer as TiO(110). In Fig. 4, (II) and (III), the PDOS of surface Ti and O atoms are plotted for the structure in Figs. 1(c) and 1(d) and a single (as cleaved) layer of TiO(110), respectively. As in the case of NiTi(001) discussed above, the PDOS curves have similar features, with comparable peak profiles, although not as striking as in Fig. 2, (II) and (III). In Figs. 1(c) and 1(d), oxygen has gained a total charge of 0.70*e* from the surface, which is close to the value 0.78*e* in the single layer of TiO(110).

The adsorption energy of atomic oxygen on NiTi(110) is 8.30 eV, which is about 0.6 eV less than for oxygen adsorbed in the fourfold hollow site on NiTi(001). Adsorption of atomic oxygen in a similar bridging site on the (110) surface of Ti is found to be exothermic by 7.84 eV. Hence, the presence of Ni atoms near the NiTi(110) surface has a stabilizing effect on the grown oxide, as found for the NiTi(001) surface.

Increasing the adsorbate coverage to 1 ML O_2 leads to the growth of one TiO_2 layer on the NiTi(110) substrate. The most stable structure that we have found is shown in Figs. 3(e) and 3(f). The adsorption energy is 7.52 eV. In this geometry, all Ti atoms in the grown oxide are fourfold coordinated, with bonds to two bridging surface O atoms (1.81 Å) and two "in-plane" O atoms (2.20 Å). The latter O atoms

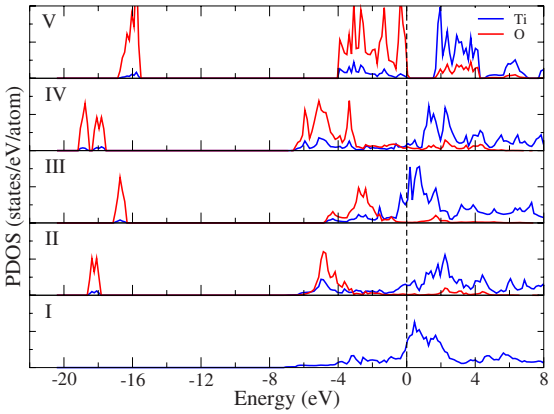

FIG. 4. (Color online) Partial density of states of Ti and O atoms: (I) clean Ti-terminated B2 NiTi(110) surface; (II) I+1 ML O adsorbed [Figs. 1(c) and 1(d)]; (III) one layer of TiO(110); (IV) I+1 ML O_2 adsorbed [Figs. 3(e) and 3(f)]; (V) one layer of TiO_2(001).

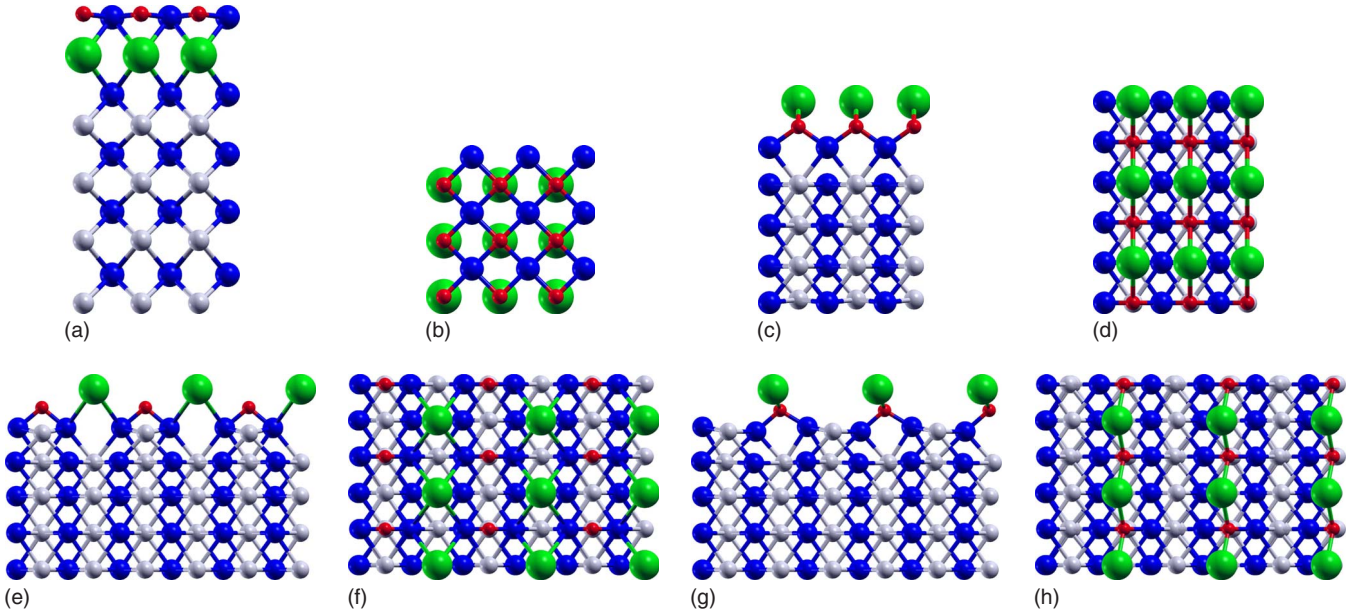

FIG. 5. (Color online) Adsorption on B2 NiTi with K doping; (a) and (b) side and top view, 1 ML O, fourfold hollow site on the (001) surface; (c) and (d) side and top view, 1 ML O , twofold bridge site on the (110) surface; (e) and (f) side and top view, 0.5 ML O, twofold bridge site on the (110) surface (2×1 supercell with only half of Ni in top layer substituted by K; K-O distance is 5.02 Å); (g) and (h) side and top view, 0.5 ML O, twofold bridge site on the (110) surface, (2×1 supercell with only half of Ni in top layer substituted by K; K-O distance is 2.57 Å). Colors (size, grayscale): K-green (huge, light gray), Ti-blue (large, gray), O-red (small, gray), Ni-white (large, white).

are also bonded to Ni (1.88 Å). As shown by Perron *et al.*,[44] the presence of Ti(4) is a signature of $TiO_2(001)$, which leads us to categorize the grown structure as $TiO_2(001)/NiTi(110)$. The calculated oxygen charges are almost identical in the geometry in Figs. 3(e) and 3(f) (0.68*e* and 0.73*e*) and in the single (as cleaved) layer of $TiO_2(001)$ (0.67*e*). In Fig. 4, (IV) and (V), the PDOS of Ti and O are plotted for $TiO_2(001)/NiTi(110)$ [Figs. 3(e) and 3(f)] and a single layer of $TiO_2(001)$, respectively. The oxygen bands below the Fermi level are shifted to lower energies in $TiO_2(001)/NiTi(110)$ compared to the single layer of $TiO_2(001)$. However, both in Fig. 4, (IV) and (V), there are overlapping oxygen bands, both at the lowest energies shown, and for energies a few electron volts below the Fermi level.

Also in this case, the surface Ti PDOS at the Fermi level diminishes upon oxidation, as expected, see Fig. 4, (I), (II), and (IV). However, the effect is less pronounced than for oxidation of the B2 (001) surface (Fig. 2). This is an indication that the coverage of 1 ML O_2 on B2 (001) yields an oxide layer which is more "bulklike" than on the B2 (110) surface. This observation is consistent with the difference in coordination of the Ti atoms in the two oxides grown: On B2 (001), the grown oxide can have either Ti(5) or Ti(6), but on B2 (110), the grown oxide has only Ti(4). The former is closer to the perfect and stoichiometric Ti(6) coordination of bulk TiO_2.

Adsorption of 1 ML O_2 on the Ti(110) surface is exothermic by only 2.60 eV. This is significantly less than for adsorption of 1 ML O, and consistent with the trend observed with the Ti(001) surface.

As expected, in most cases, the adsorption energy increases when the oxygen coverage is reduced to submonolayer values. This can be ascribed to a reduction in repulsive interactions between the adsorbed oxygen atoms. The changes in E_{ads} seem to correlate well with the "oxygen density" on the surface, which decreases in the order O_2 on B2 (001), O_2 on B2 (110), O on B2 (001), and O on B2 (110). The corresponding changes in E_{ads} are 2.59, 2.04, −0.39, and −0.66 eV (see Table I). Note that these numbers are based on a comparison of ADF/BAND adsorption energies for (1×1) supercells and DACAPO adsorption energies for (2×1) supercells. Test calculations with DACAPO on a few of the (1×1) supercells indicate that these adsorption energy changes are somewhat too low, by about 0.5 eV, but the observed trend should be reliable.[46]

3. Effect of potassium doping of B2 NiTi (001) and (110)

In the experiments reported by Tollefsen *et al.*,[8] nitinol samples with submonolayer (about 0.3 ML) coverage of K were studied. Our goal here is to address the influence of the presence of K atoms on the oxidation of NiTi surfaces. To enable valid comparisons with the results obtained for oxidation of undoped NiTi, we have chosen to model the K doping by replacing near surface Ni atoms with K atoms in the five layer slab structures discussed in the previous section. In the typical case, the (1×1) slab supercell is retained by replacing one of the five Ni atoms by K. This corresponds to a coverage of 1 ML K. However, we have also modeled 0.5 ML coverage of K by using a (2×1) slab supercell and replacing only one of the two near surface Ni atoms by K. For simplicity, we will refer to the replacement of Ni atoms by K as "K doping" and the corresponding slab structures as "K-doped" surfaces. This terminology is also used in the relevant literature.[8]

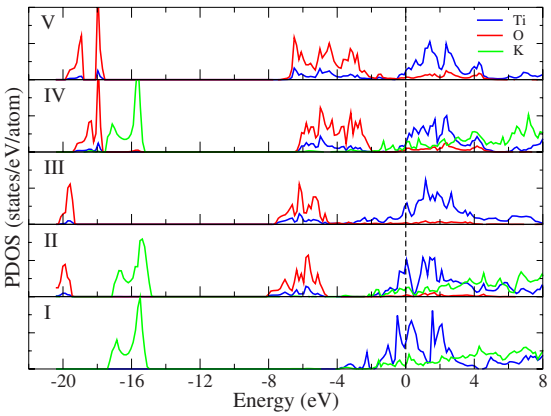

FIG. 6. (Color online) Partial density of states (B2 (001)) of Ti, O, and K atoms: (I) clean K-doped NiTi(001); (II) I+1.0 ML O adsorbed [Figs. 5(a) and 5(b)]; (III) 1.0 ML O adsorbed on NiTi(001) [Figs. 1(a) and 1(b)]; (IV) I+1 ML O_2 adsorbed [Figs. 7(a) and 7(b)]; V) 1 ML O_2 adsorbed on NiTi(001) [Figs. 3(c) and 3(d)].

The Ti-terminated K-doped (001) surface of B2 NiTi is structurally similar to the undoped surface, and as expected, the favored site for adsorption of atomic oxygen is the fourfold hollow site, as found with the undoped surface. The resulting geometry, with a coverage of 1 ML O, is shown in Figs. 5(a) and 5(b), and should be compared with the corresponding undoped structure in Figs. 1(a) and 1(b). The effects of K doping are a reduction in the Ti-O bond from 2.09 Å to 2.06 Å, and an increase in the oxygen charge from 0.88*e* to 0.98*e*. The adsorption energy increases, from 8.87 eV to 9.67 eV, indicating that the presence of K facilitates the growth of an oxide layer on the substrate surface. With reference to the discussion of the undoped case above, the structure in Figs. 5(a) and 5(b) is categorized as TiO(001)/KNiTi(001).

Increasing the adsorbate coverage to 1 ML O_2 results in low energy K-doped structures similar to the undoped versions of Figs. 3(a)–3(d). The geometry analogous to Figs. 3(c) and 3(d) is shown in Figs. 7(a) and 7(b), where one O is located in the fourfold hollow site and the other in a bridging position between two Ti atoms [cf. Figs. 3(c) and 3(d)]. The Ti-O bonds are 2.14 and 1.59 Å, and the oxygen charges are 0.87*e* and 0.60*e* for the O atom in the fourfold hollow site and in the bridging position, respectively. These values are almost the same as without K doping [Figs. 3(c) and 3(d)]. However, the adsorption energy of 9.68 eV is about 1.5 eV larger than without K doping. As found for adsorption of 1 ML O, it is evident that the presence of K, also with 1 ML O_2, has a positive effect on the formation of the oxide layer. The similarity between Figs. Figs. 7(a) and 7(b) and 3(c) and 3(d) suggests a categorization of the former as TiO_2(110)/KNiTi(001). The K-doped analogy of the structure in Figs. 3(a) and 3(b) has Ti-O bond lengths and oxygen charges very similar to the undoped structure. The adsorption energy is 9.47 eV, which is about 1.5 eV more than without K doping. This structure (not shown here) is categorized as TiO_2(100)/KNiTi(001), in analogy with the structure in Figs. 3(a) and 3(b).

The similarities between the undoped and K-doped structures discussed above are reflected also in the Ti and O PDOS curves, as shown in Fig. 6, (II)–(V). There are only minor changes in the band widths and positions as a result of the K doping, both with a coverage of 1 ML O [Fig. 6, (II) vs Fig. 6, (III)] and with a coverage of 1 ML O_2 [Fig. 6, (IV) vs Fig. 6, (V)]. As expected, the surface Ti PDOS at the Fermi level is reduced upon oxidation, also for the K-doped (001) surface [see Fig. 6, (I), (II), and (IV)] but to a lesser extent than for the undoped B2 (001) surface.

Replacement of the near surface Ni atom by K in the (110) surface of B2 NiTi results, upon geometry relaxation, in a structure which is markedly different from the undoped (110) surface. In the undoped case, the Ti atoms move out and the Ni atoms move in, when compared with the as cleaved (bulklike) (110) NiTi layers. With Ni replaced by K, the K atoms move out and the Ti atoms move in. This is essentially caused by the K atoms having a much larger radius than Ni.

With such a K-terminated (110) surface as the "reactant," oxygen atoms can be adsorbed in a variety of sites, both above and below the K atoms. The lowest energy configurations have oxygen below the surface layer of K atoms, enabling the formation of a TiO or TiO_2 layer, depending on the oxygen coverage.

At a coverage of 1 ML O, the favored adsorption site on KNiTi(110) is in the bridging site between two Ti atoms, see Figs. 5(c) and 5(d). This geometry is similar to the corresponding undoped structure shown in Figs. 1(c) and 1(d), and therefore categorized as TiO(110)/KNiTi(110). However, each O atom is now also bonded to two K atoms, resulting in a longer Ti-O bond length, 1.91 vs 1.84 Å, and a higher oxygen charge, 0.91*e* vs 0.70*e*, when we compare with the undoped case, Figs. 1(c) and 1(d). The adsorption energy for the structure in Figs. 5(c) and 5(d) is 9.23 eV, which is almost 1 eV higher than the undoped version in Figs. 1(c) and 1(d). Again, the presence of potassium has a stabilizing effect on the grown oxide layer.

At a coverage of 1 ML O_2 on KNiTi(110), the energetically most favored structure has a TiO_2(001)-like oxide layer below the surface layer of K atoms. This geometry is essentially obtained from the one discussed above, Figs. 5(c) and 5(d), by adding an oxygen atom to a "vacant site" in the uppermost Ti layer, on top of Ti in the layer below. The resulting structure is shown in Figs. 7(c) and 7(d). The Ti-O bonds are 2.13 Å (in plane) and 1.90 Å (vertically) for the threefold coordinated oxygen atom added to the vacant site. For the O atom in the bridging site between two Ti atoms, and also with bonds to two K atoms, the Ti-O bond length is 1.91 Å, i.e., the same as for the corresponding O atom in Figs. 5(c) and 5(d). The total charge on the two O atoms is 1.75*e*, which is partly donated by Ti atoms in the upper two layers, and partly by the K atoms on the surface. The adsorption energy for the structure in Figs. 7(c) and 7(d) is 10.94 eV, which is 3.4 eV higher than for the structure in Figs. 3(e) and 3(f), which represents the undoped version of 1 ML O_2 on B2 NiTi(110). Clearly, the K doping has made possible a particularly stable layer of TiO_2.

In Fig. 8, the electronic structures of K-doped and undoped versions of oxidized B2 NiTi(110) are compared in terms of PDOS curves for Ti, O, and K. The similarities between TiO(110)/KNiTi(110), Figs. 5(c) and 5(d), and

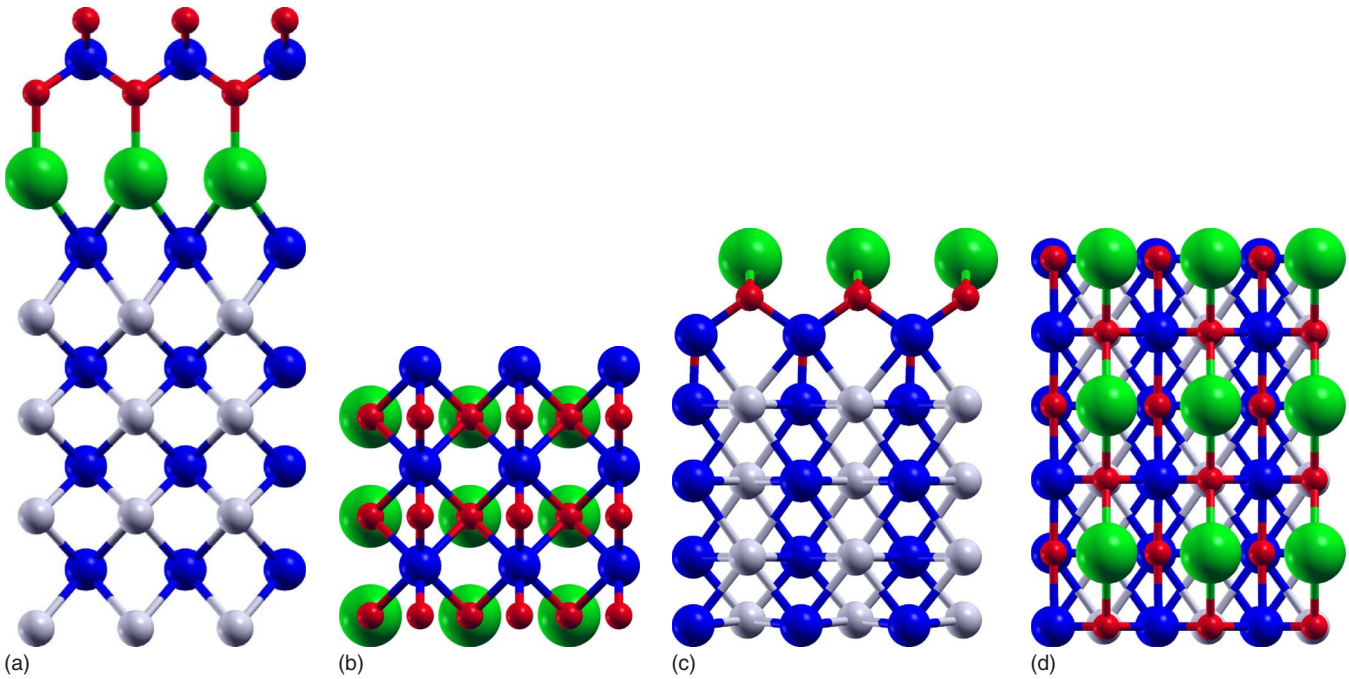

FIG. 7. (Color online) Adsorption of 1 ML O_2 on B2 NiTi with K doping; (a) and (b) side and top view, hollow and bridge sites on the (001) surface; (c) and (d) side and top view, bridge and in-plane sites on the (110) surface. Colors (size, grayscale): K-green (huge, light gray), Ti-blue (large, gray), O-red (small, gray), Ni-white (large, white).

TiO(110)/NiTi(110), Figs. 1(c) and 1(d), are reflected in Ti and O PDOS curves in Fig. 8, (II) and (III) sharing several common features. Further, based on the discussion above, the K-doped structure with 1 ML O_2 adsorbed, Figs. 7(c) and 7(d), can be related both to the K-doped structure with 1 ML O adsorbed, Figs. 5(c) and 5(d), and to the undoped structure with 1 ML O_2 adsorbed, Figs. 3(e) and 3(f). This is reflected in the PDOS curves of Fig. 8, (IV) having common features with the corresponding curves in *both* Fig. 8, (II) and (V). A comparison of Fig. 8, (I), (II), and (IV) shows a reduced value of the surface Ti PDOS at the Fermi level upon oxidation of the surface. However, the Ti PDOS reduction is more pronounced for the undoped surface.

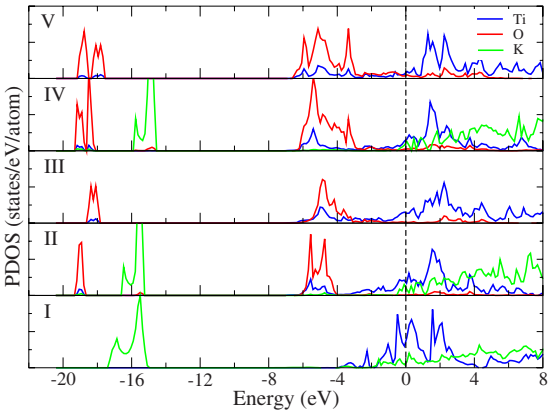

FIG. 8. (Color online) Partial density of states (B2 (110)) of Ti, O, and K atoms; (I) clean K-doped NiTi(110); (II) I+1 ML O adsorbed [Figs. 5(c) and 5(d)]; (III) 1 ML O adsorbed on NiTi(110) [Figs. 1(c) and 1(d)]; (IV) I+1 ML O_2 adsorbed [Figs. 7(c) and 7(d)]; (V) 1 ML O_2 adsorbed on NiTi(110) [Figs. 3(e) and 3(f)].

For the K-doped B2 NiTi(110) surface, we find interesting differences in the adsorption energy at submonolayer oxygen coverage, depending on the relative positions of the oxygen and potassium atoms. For the geometry shown in Figs. 5(e) and 5(f), the adsorption energy is 7.35 eV. Here, the distance between K and O atoms is large, and the stabilizing effect of K on the grown oxide layer is absent. However, as is evident from the top view in Fig. 5(f), the O atom could alternatively be located in a Ti-O-Ti bridging position between two K atoms. In this alternative geometry, see Figs. 5(g) and 5(h), the positive influence of the K atoms is reflected in a much higher adsorption energy of 8.99 eV.

B. Adsorption of oxygen on the *B19′* phase of NiTi

1. Bulk B19′ *NiTi and its low index surfaces*

For the monoclinic B19′ phase of NiTi, we have used experimentally determined values for the lattice parameters, a=2.89 Å, b=4.62 Å, c=4.12 Å, and γ=96.8°.[47] There has been a lack of consensus in the literature on the position of atoms in the unit cell,[48,49] although the lattice parameters are all in good agreement. This inconsistency has been noted over the last few decades.[47] In this study, we have chosen the atomic positions described by Kulkova *et al.*[48] and consider oxygen adsorption on the (010) surface, which is found to have a lower energy than the (001) and (100) surfaces.[11]

The as cleaved (010) surface consists of equal amounts of Ni and Ti atoms, and upon relaxation of the geometry, the Ti atoms move out and the Ni atoms move in, creating an essentially Ti-terminated surface. As such, the (010) surface of B19′ is similar to the (110) surface of the B2 phase.

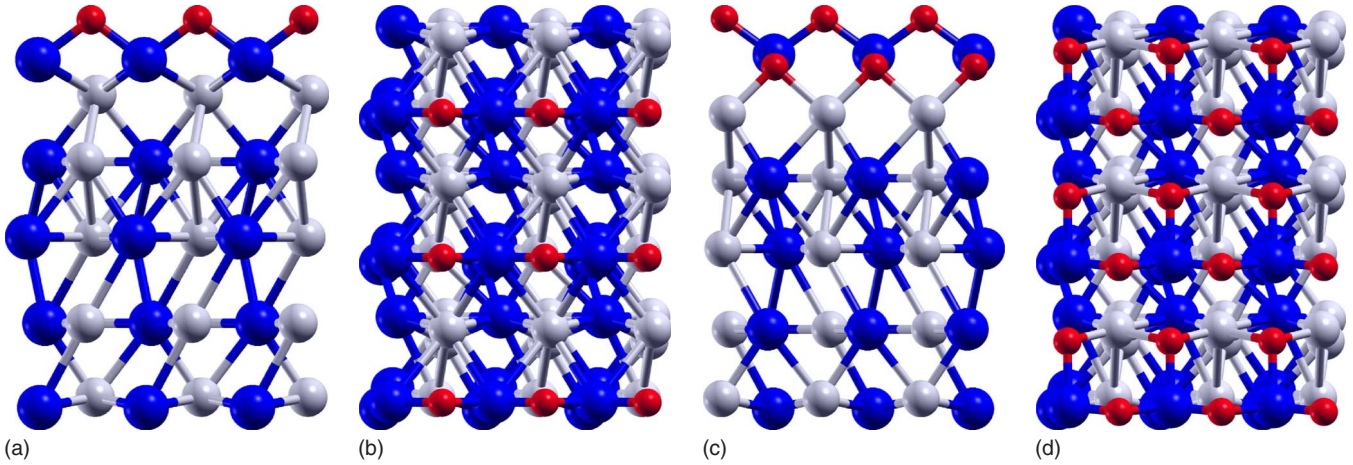

FIG. 9. (Color online) Adsorption of oxygen on B19′ NiTi(010); (a) and (b) side and top view, 1 ML O, twofold bridge site; (c) and (d) side and top view, 1 ML O_2, bridge and in-plane sites. Colors (size, grayscale): Ti-blue (large, gray), O-red (small, gray), Ni-white (large, white).

2. Oxygen adsorption on undoped B19′ NiTi (010)

Oxygen adsorbs at a bridge site between two Ti atoms, corresponding to 1 ML O coverage, as shown in Figs. 9(a) and 9(b). One layer of TiO(110) is formed on the substrate surface, similar to the growth on the NiTi(110) surface in the B2 phase. The Ti-O bond length of 1.83 Å is almost the same as the value of 1.84 Å for TiO(110)/NiTi(110), Figs. 1(c) and 1(d). The adsorbed oxygen atom has gained a charge of 0.65*e*, which is similar to adsorption of 1 ML O on the B2 (110) surface. However, there appears to be a larger contribution of charge transfered from the Ni atoms to O in TiO(110)/NiTi(010) than in TiO(110)/NiTi(110). Based on the Ti and O PDOS curves in Fig. 4, (II) and Fig. 10, (II), we conclude that these two geometries have a similar electronic structure at the surface. Also, the adsorption energy of 8.01 eV for TiO(110)/NiTi(010) is similar to 8.30 eV found for TiO(110)/NiTi(110).

Increasing the oxygen coverage to 1 ML O_2 results in the growth of a TiO_2(001)-like oxide layer, shown in Figs. 9(c) and 9(d). All Ti atoms in the grown oxide are fourfold coordinated, with bonds to two bridging surface O atoms (1.79 Å) and two in-plane O atoms (2.05 Å). The total charge gained by the two oxygen atoms is 1.42*e*, and the adsorption energy is 7.49 eV, to be compared with 1.41*e* and 7.52 eV found for adsorption of 1 ML O_2 on the B2 (110) surface [Table I and Figs. 3(e) and 3(f)]. We also note that a reduction to submonolayer oxygen coverage (0.5 ML O) on the B19′ (010) surface results in an increased adsorption energy (see Table III), similar to the behavior of the B2 (110) surface (see Table I).

The electronic structure of undoped B19′ (010), with and without oxygen adsorbed, is visualized in terms of Ti and O PDOS curves in Fig. 10, (I)–(III). Comparison should be made with the corresponding PDOS curves for the B2 (110) surface, Fig. 4, (I), (II), and (IV). Note, again, that the surface Ti PDOS at the Fermi level is reduced upon oxygen adsorption, in particular at high oxygen coverage (i.e., 1 ML O_2).

3. Effect of potassium doping of B19′ NiTi (010)

Replacement of the near surface Ni atom by K in the (010) surface of B19′ NiTi results in K moving out of and Ti moving into the surface, similar to what was found with the B2 (110) surface. The energetically favored geometries upon adsorption of 1 ML O and 1 ML O_2 have their natural B2 (110) counterparts. This is apparent if one compares the structure in Figs. 11(a) and 11(b), B19′ KNiTi(010)+O, with the one in Figs. 5(c) and 5(d), B2 KNiTi(110)+O, and the structure in Figs. 11(c) and 11(d), B19′ KNiTi(010)+O_2, with the one in Figs. 7(c) and 7(d), B2 KNiTi(110)+O_2. Values for adsorption energies and oxygen charges are comparable, see Tables IV and II. Also for the B19′ (010) surface, the K doping results in significantly higher adsorption energies than for the undoped NiTi surface. At a coverage of 1 ML O, E_{ads} increases from 8.01 eV (undoped) to 9.00 eV (K-doped), and at a coverage of 1 ML O_2, E_{ads} increases

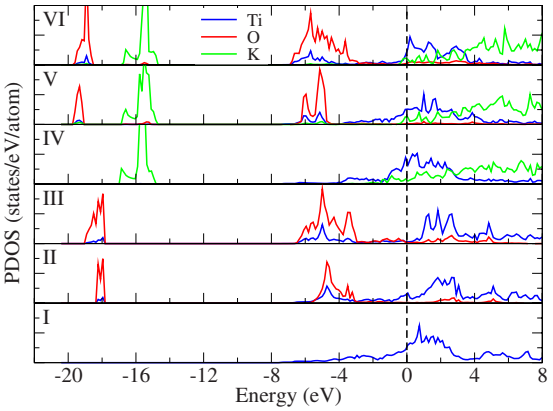

FIG. 10. (Color online) Partial density of states (B19′ phase) of Ti, O, and K atoms; (I) clean NiTi(010); (II) I+1 ML O adsorbed [Figs. 9(a) and 9(b)]; (III) I+1 ML O_2 adsorbed [Figs. 9(c) and 9(d)]; (IV) clean K-doped NiTi(010); (V) IV+1 ML O adsorbed [Figs. 11(a) and 11(b)]; (VI) IV+1 ML O_2 adsorbed [Figs. 11(c) and 11(d)].

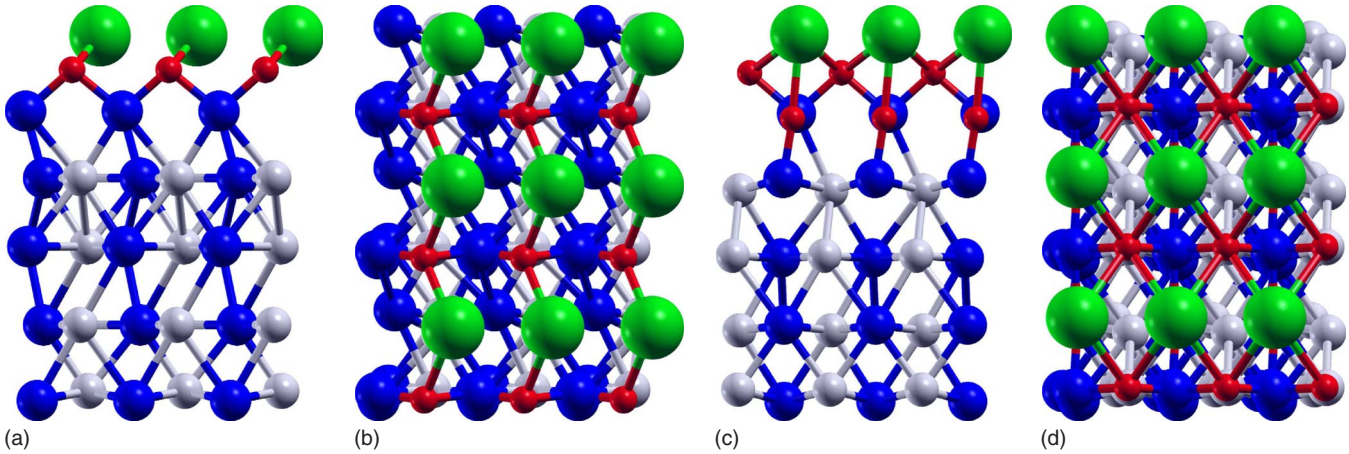

FIG. 11. (Color online) Adsorption of oxygen on K-doped B19′ NiTi(010); (a) and (b) side and top view, 1 ML O, twofold bridge site; (c) and (d) side and top view, 1 ML O_2, bridge and in-plane sites. Colors (size, grayscale): K-green (huge, light gray), Ti-blue (large, gray), O-red (small, gray), Ni-white (large, white).

from 7.49 eV (undoped) to 12.63 eV (K-doped).

The electronic structure of K-doped B19′ (010), with and without oxygen adsorbed, is visualized in terms of Ti, O, and K PDOS curves in Fig. 10, (IV)–(VI). Comparison should be made with the corresponding PDOS curves for the K-doped B2 (110) surface, Fig. 8, (I), (II), and (IV). The surface Ti PDOS at the Fermi level is somewhat reduced upon oxygen adsorption but to a much lesser extent than for the undoped B19′ (010) surface.

IV. DISCUSSION

As pointed out in the previous section, the PDOS calculations, as presented in Figs. 2, 4, 6, 8, and 10, show that the formation of TiO and TiO_2 results in a lower Ti PDOS at the Fermi level compared to the clean surface, with the Ti PDOS corresponding to TiO_2 formation being the lowest. In general, a low density of states at the Fermi level is related to high stability.[49,50] The Ti PDOS at the Fermi level is less reduced for the K-doped surfaces than for the undoped surfaces, in particular for B2 (110) and B19′ (010). This indicates that the K-doped surfaces are more reactive toward additional oxygen and have the best potential for growing thicker oxide layers.

Upon oxidation of the NiTi surfaces, the vertical separation between the outermost Ti layer and the Ni layer below increases in most cases. This is a sign of depletion of Ni atoms from the surface region, consistent with a previous study.[51] In Fig. 12, we have plotted the change in this vertical Ti-Ni separation upon oxide formation. The depletion of Ni from the surface is most pronounced upon the formation of TiO_2, corresponding to two O atoms pr surface Ti atom. From Fig. 12, the effect appears to be larger for the undoped surfaces (solid lines) than for the K-doped surfaces (dashed lines). However, one should keep in mind that the Ti-Ni separation prior to oxidation is significantly larger for the K-doped than for the undoped surfaces. This is mainly because replacement of near surface Ni atoms with K trivially removes Ni atoms from the surface region. In any case, it is fair to say that K doping and oxide formation both contribute to the depletion of Ni atoms from the surface.

Even with undoped NiTi surfaces, our calculations suggest that O_2 dissociates with practically no energy barrier. Upon K doping, the adsorption energies increase (Table II vs Table I, Table IV vs Table III), and the Ti-O bond distances are closer to the values in bulk TiO_2. Thus, the catalytic role played by the K atoms, for the enhancement of the stability of the grown oxide layer, appears to be via electron donation to the oxygen atoms, and not by a reduction in the energy barrier of dissociation.

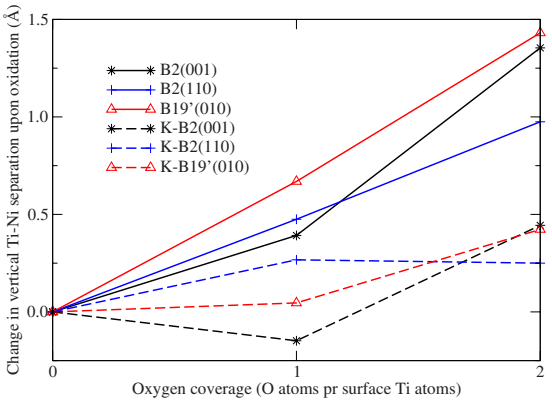

FIG. 12. (Color online) Oxygen coverage dependence of the relaxation of surface atoms for undoped (solid lines) and K-doped (dashed lines) surfaces of B2 (001) (black), B2 (110) (blue), and B19′ (010) (red), i.e., change in vertical Ti-Ni separation upon oxidation. At 1 ML O coverage (one O pr surface Ti), the data points correspond to the geometries of Figs. 1(a) and 1(b) (black star, solid), 1(c) and 1(d) (blue plus, solid), 9(a) and 9(b) (red triangle, solid), 5(a) and 5(b) (black star, dashed), 5(c) and 5(d) (blue plus, dashed), 11(a) and 11(b) (red triangle, dashed). At 1 ML O_2 coverage (two O pr surface Ti), the data points correspond to the geometries of Figs. 3(c) and 3(d) (black star, solid), 3(e) and 3(f) (blue plus, solid), 9(c) and 9(d) (red triangle, solid), 7(a) and 7(b) (black star, dashed), 7(c) and 7(d) (blue plus, dashed), 11(c) and 11(d) (red triangle, dashed).

The present study is limited to the growth of a single layer of TiO_2. As shown in Fig. 12, the geometric relaxation effects increase with increasing oxygen coverage. Presumably, two to three oxide layers could grow, but additional growth is not expected to make a big difference, since it has been found that O_2 physisorbs on $TiO_2(110)$ once it has fully resumed its passivating role.[52] The surface treatment by K doping represents a real possibility to obtain more than a single layer of Ti atoms at the surface, thereby enabling the formation of, say, two to three layers of TiO_2 outside the outermost Ni atoms. Clearly, this would require the adsorption of at least 2–3 ML of O_2. Our ambition here has not been to establish a mechanism for how Ni atoms near the surface are replaced by K atoms but rather to identify the resulting geometries, assuming the replacement has taken place.

The XPS experiments reported by Tollefsen *et al.*[8] show that K doping enhances the formation of TiO_2 at the expense of lower oxides, e.g., TiO. Our results are in agreement with this observation, since the adsorption energies E_{ads} increase significantly more upon K doping for the formation of TiO_2 than for the formation of TiO. The effect is more pronounced for the B19′ (010) surface (0.99 eV vs 5.14 eV) and the B2 (110) surface (0.93 eV vs 3.42 eV) than for the B2 (001) surface (0.80 eV vs 1.51 eV). Here, the numbers in parenthesis represent the increase in E_{ads} upon K doping for TiO and TiO_2 formation, respectively (see Tables I–IV).

TiO_2 is experimentally known to exhibit stable surface indexes including rutile $TiO_2(110)$, rutile $TiO_2(101)$, and anatase $TiO_2(101)$.[13,53] The former is the most stable. NiTi(001) and NiTi(110) of the B2 phase, and NiTi(010) of the B19′ phase are the most investigated NiTi surfaces in previous studies[11,18] because of their high stability, which is also found in the present study. We have considered these three surfaces of NiTi since it is important to identify which titanium oxide that will grow on which substrate surface. Indeed, our investigation shows that the TiO_2 growth on the B2 NiTi(001) surface is best categorized as rutile $TiO_2(110)$ [Figs. 3(c) and 3(d)] or $TiO_2(100)$ [Figs. 3(a) and 3(b)]. As shown by Perron *et al.*[44] these two surfaces of rutile are structurally rather similar. On the other hand, the oxide growth on NiTi(110) in the B2 phase and NiTi(010) in the B19′ phase is better categorized as rutile $TiO_2(001)$. It has been shown[44] that rutile $TiO_2(001)$ is of lower stability than $TiO_2(101)$, which in turn is less stable than $TiO_2(100)$. Doping of the NiTi alloy with K atoms does not change this growth pattern for the different surfaces. As discussed already, $TiO_2(001)$ is characterized by fourfold coordinated Ti atoms, whereas $TiO_2(110)$ and $TiO_2(100)$ have sixfold- and fivefold-coordinated Ti atoms. Since bulk rutile has sixfold-coordinated Ti atoms, we expect a fully passivating oxide to be obtained with about two layers of TiO_2 on B2 NiTi(001), and with slightly more, about three layers of TiO_2, on B2 NiTi(110) and B19′ NiTi(010).

V. CONCLUSION

The main results and implications of the present study can be summarized as follows: (1) NiTi surface alloys react with oxygen and form stable titanium oxides, with adsorption energies in the range 7–11 eV pr adsorbed atom or molecule, as predicted by DFT calculations. (2) Based on their geometric and electronic structures, the grown TiO and TiO_2 surface layers are conveniently categorized in terms of specific low-index surfaces of these oxides. (3) Both TiO and TiO_2 promote the biofunctionality of NiTi surface alloys by depleting Ni atoms from the surface region. (4) By the growth of TiO_2, increased stability of the oxide and biofunctionality of the NiTi surface is obtained. (5) Doping of the NiTi alloy, i.e., replacement of near surface Ni with K atoms, improves the strength of the grown oxides, enhances the formation of TiO_2 at the expense of TiO, and represents a surface treatment mechanism that enables two or more successive layers of Ti atoms at the surface, and thereby the possibility of growing thicker passivating layers of TiO_2.

ACKNOWLEDGMENTS

We thank S. Raaen and H. Tollefsen for fruitful discussions. NOTUR is acknowledged for providing computer time.

*Corresponding author; jon.stovneng@ntnu.no

[1] D. Brunette, P. Tengvall, M. Textor, and P. Thomsen, *Titanium in Medicine* (Springer-Verlag, Berlin, 2001).
[2] K. Otsuka and C. Wayman, *Shape Memory Materials* (Cambridge University Press, UK, 2002).
[3] C. Leyens and M. Peters, *Titanium and Titanium Alloys, Fundamentals and Applications* (Wiley-VCH, Weinheim, 2003).
[4] G. Andreasen, Am. J. Orthod. **78**, 528 (1980).
[5] M. Simon, C. Athanasoulis, D. Kim, F. L. Steinberg, D. H. Porter, B. H. Byse, S. Kleshinski, S. Geller, D. E. Orron, and A. C. Waltman, Radiology **172**, 99 (1989).
[6] H. Gerber and S. Perren, in *Evaluation of Biomaterials*, edited by G. D. Winter, J. L. Leray, and K. de Groot (Wiley, New York, 1980).
[7] L. Peltonen, Contact Dermatitis **5**, 27 (1979).
[8] H. Tollefsen and S. Raaen, J. Appl. Phys. **105**, 123501 (2009).
[9] C. Chu, S. Wu, and Y. Yen, Mater. Sci. Eng., A **216**, 193 (1996).
[10] L. Zhang, C. Xie, and J. Wu, Mater. Charact. **58**, 471 (2007).
[11] S. Kulkova, V. Egorushkin, S. Eremeev, and S. Kulkov, Mater. Sci. Eng., A **438-440**, 476 (2006).
[12] A. Michiardi, C. Aparicio, J. Planell, and F. Gil, Surf. Coat. Technol. **201**, 6484 (2007).
[13] C. Chu, T. Hu, S. Wu, Y. Dong, L. Yin, Y. Pu, P. Lin, C. Chung, K. Yeung, and P. Chu, Acta Biomater. **3**, 795 (2007).
[14] J. Ryhänen, M. Kallioinen, J. Tuukkanen, P. Lehenkari, J. Junila, E. Niemela, P. Sandvik, and W. Serlo, Biomaterials **20**, 1309 (1999).
[15] Y. Fu, W. Huang, H. Du, X. Huang, J. Tan, and X. Gao, Surf. Coat. Technol. **145**, 107 (2001).
[16] F. Wang, W. Buehler, and S. Pickart, J. Appl. Phys. **36**, 3232

(1965).
[17] A. Kellou, Z. Nabi, A. Tadjer, N. Amrane, N. Fenineche, and H. Aourag, Phys. Status Solidi B **239**, 389 (2003).
[18] S. Kulkov, S. Eremeev, and S. Kulkova, Phys. Solid State **51**, 1281 (2009).
[19] W. Cai, C. Tan, T. Shen, and X. Tian, J. Alloys Compd. **438**, 30 (2007).
[20] E. Goo and R. Sinclair, Acta Metall. **33**, 1717 (1985).
[21] M. Punkkinen, K. Kokko, and I. Vayrynen, Solid State Commun. **108**, 567 (1998).
[22] Y. Teng, S. Zhu, F. Wang, and W. Wu, Physica B **393**, 18 (2007).
[23] C. Tan, W. Cai, and J. Zhu, Phys. Status Solidi B **243**, R69 (2006).
[24] P. Soukiassian, T. Gentle, M. Bakshi, and Z. Hurych, J. Appl. Phys. **60**, 4339 (1986).
[25] M. Nolan and S. Tofail, Biomaterials **31**, 3439 (2010).
[26] M. Nolan and S. Tofail, Phys. Chem. Chem. Phys. **12**, 9742 (2010).
[27] S. Vosko, L. Wilk, and M. Nusair, Can. J. Phys. **58**, 1200 (1980).
[28] J. P. Perdew, J. A. Chevary, S. H. Vosko, K. A. Jackson, M. R. Pederson, D. J. Singh, and C. Fiolhais, Phys. Rev. B **46**, 6671 (1992).
[29] http://www.scm.com
[30] G. te Velde and E. J. Baerends, Phys. Rev. B **44**, 7888 (1991).
[31] P. H. T. Philipsen, E. van Lenthe, J. G. Snijders, and E. J. Baerends, Phys. Rev. B **56**, 13556 (1997).
[32] G. Wiesenekker and E. J. Baerends, J. Phys.: Condens. Matter **3**, 6721 (1991).
[33] The KSPACE parameter denotes the number of sample points from the Γ point to a vertex of the Brillouin zone, including the two end points. For a square Brillouin zone, then, one has at the outset a 9×9 regular square lattice of k points, out of which only the symmetry unique points are selected.
[34] K. Yamaguchi, F. Jensen, A. Dorigo, and K. Houk, Chem. Phys. Lett. **149**, 537 (1988).
[35] C. Schweitzer and R. Schmidt, Chem. Rev. **103**, 1685 (2003).
[36] http://dcwww.fysik.dtu.dk/campos/Dacapo
[37] D. Vanderbilt, Phys. Rev. B **41**, 7892 (1990).
[38] Note that the slab-to-slab interaction is not an issue in the ADF/BAND program, where the slab is a truly 2D system which is not repeated in the third dimension.
[39] H. J. Monkhorst and J. D. Pack, Phys. Rev. B **13**, 5188 (1976).
[40] F. Birch, J. Geophys. Res. **83**, 1257 (1978).
[41] O. Mercier, K. Melton, G. Gremaud, and J. Hägl, J. Appl. Phys. **51**, 1833 (1980).
[42] G. Bihlmayer, R. Eibler, and A. Neckel, Phys. Rev. B **50**, 13113 (1994).
[43] R. Weast and M. Astle, *CRC Handbook of Chemistry and Physics* (CRC Press, Boca Raton, Florida, 1982).
[44] H. Perron, C. Domain, J. Roques, R. Drot, E. Simoni, and H. Catalette, Theor. Chem. Acc. **117**, 565 (2007).
[45] At lower oxygen coverage, a structure with the O atom in a bridge between Ti and Ni is also possible, as shown by Nolan *et al.* (Ref. 25). At a coverage of 1 ML O, this is not an energy minimum. However, a structure with the Ti-O-Ti bridge and an O-Ni bond in addition is possible, also at a coverage of 1 ML O. The energy of this structure is very close to the one discussed here [Figs. 1(c) and 1(d)].
[46] For adsorption of 1 ML O and 1 ML O_2 on B2 NiTi(001), DACAPO gives E_{ads}=8.06 eV and 7.92 eV, which is, respectively, 0.81 eV and 0.25 eV less than obtained with the ADF/BAND program.
[47] G. Michal and R. Sinclair, Acta Crystallogr., Sect. B: Struct. Crystallogr. Cryst. Chem. **37**, 1803 (1981).
[48] S. Kulkova, V. Egorushkin, S. Eremeev, J. Kim, G. Lee, and Y. Koo, Physica B **349**, 342 (2004).
[49] G. Bihlmayer, R. Eibler, and A. Neckel, J. Phys.: Condens. Matter **5**, 5083 (1993).
[50] Y. Y. Ye, C. T. Chan, and K. M. Ho, Phys. Rev. B **56**, 3678 (1997).
[51] P. Filip, J. Lausmaa, J. Musialek, and K. Mazanec, Biomaterials **22**, 2131 (2001).
[52] Z. Dohnálek, J. Kim, O. Bondarchuk, J. M. White, and B. D. Kay, J. Phys. Chem. B **110**, 6229 (2006).
[53] C. Chu, C. Chung, and P. Chu, Mater. Sci. Eng., A **417**, 104 (2006).